

# Quantum Efficiency of backside-illuminated pixels under ultraviolet illumination: ARC coatings impact measurements and simulations

Nour Fassi\*†, Jean-Pierre Carrère\*, Pierre Magnan†, Magali Estribeau†, Vincent Goiffon†

Email : {nour.fassi, jean-pierre.carrere}@st.com {pierre.magnan, magali.estribeau, vincent.goiffon}@isae-superaero.fr

\* ST Microelectronics, Crolles, France

†Image Sensor Research Team, ISAE-SUPAERO, Université de Toulouse, Toulouse, France

## Abstract

Up to now, backside illuminated (BSI) CMOS miniaturized pixels have been developed and manufactured for visible (Vis) and/or near infrared (NIR) light. This work focuses on the performance of these BSI CMOS miniaturized pixels, under UV light and more precisely in the range of [200 nm, 400 nm], which have been understudied until now.

This performance evaluation is based on quantum efficiency (QE) measurements of various pixel types to examine how much the good signal-to-noise ratio (SNR) in the Vis may be modified in the UV spectrum. The pixels studied here are all miniaturized backside illuminated (BSI) CMOS because they have a better light to charge conversion compared to their frontside illuminated counterparts: the architecture offers the advantage of direct access to the Si substrate and a variety of possible thinner antireflection coating (ARC) stacks thanks to the evolution of CMOS BSI passivation techniques. Optical simulations have been performed to identify the key parameters that could play a role in the pixel's improved response to the UV. Despite the lack of any process optimization, we can observe a significant response from the sensor under UV.

Keywords—ultraviolet, backside illuminated pixels, CMOS image sensors, antireflective coatings, quantum efficiency

## Introduction

Ultraviolet light detection [10 nm, 400 nm] is of particular interest in several applications such as security, authentication, criminalistics, healthcare monitoring, and environmental hazard detection (e.g.: for the invisible hazardous gases like hydrogen, a flammable gas that is hardly detectable in the visible range) [1]. In this paper, we focus only on the [200 nm, 400 nm] range to avoid photoionization, which occurs below 180 nm and induces additional difficulty in radiation manipulation [2].

To be able to detect UV, several challenges need to be addressed. As the absorption of UV light in silicon does occur in less than 10 nm, as shown in Fig.1, the passivation of the backside interface is important and even crucial to prevent recombination and other interface defects. This passivation stack is also used as an ARC so UV absorption has to be minimized in this layer.

Different approaches and methodologies have been found in the literature to improve passivation and UV light sensitivity of CCD or CMOS pixels. The first passivation technique for CCD

used molecular beam epitaxy (MBE) to grow a thin, heavily boron-doped layer [3]. Nowadays, BSI passivation is done by improved MBE growth (oxide bonding, delta doping) to enable high QE in the UV spectrum for CCDs [4] [5], or with field-effect passivation for BSI CMOS pixels, the technique used for our pixels of interest [6].

In this work, several miniaturized BSI CMOS image sensors, initially developed for the Vis and/or NIR range, are evaluated under UV light. The goal is to identify the technological parameters impacting the QE at short wavelengths and identify the elements to improve to develop an optimized pixel for UV light from existing technologies.

The passivation is performed using charged stacks of dielectrics (ARC): a positive charged oxide-nitride-oxide (ONO) stack for p-type pixels, which need an electron filled interface, and a negative charged high-k stack (with high dielectric constant materials, mainly  $\text{TA}_2\text{O}_5$  and  $\text{Al}_2\text{O}_3$ ), for n-type pixels [7]. Those ARCs have an optical and electrical impact on the pixel's performance which must be evaluated. The type of photodiode used, planar or photogate, as well as the presence of microlens may have an impact on the response of pixels under UV.

The objective of our study is to study how the various ARC stacks behave under UV illumination, for different types of photodiodes.

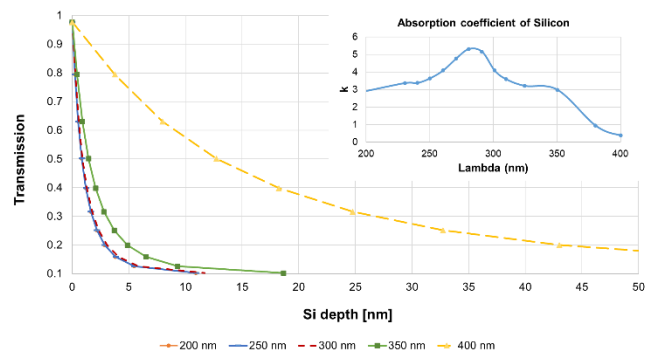


Figure 1 Beer-Lambert law: transmission depending on the penetration depth in the silicon for several UV wavelengths, and absorption coefficient of Si measured by ellipsometry.

To do so, Lumerical simulations of the optical transmittance of the ARC stacks have been performed, and the quantum efficiencies of the different pixels have been measured under UV.

## Experimental

### Investigated BSI devices

Four different samples, all miniaturized BSI CMOS, have been studied. The pixel characteristics (pitch, wafer type, and photoelement) are different for each sample. Moreover, various ARC stack compositions and thicknesses have been investigated (Table 1).

**Table 1: Pixels characteristics**

Sample	Pitch [μm]	Collected carrier	Photodiode	ARC stack [nm]	μlens
1	3.2	n-type (e <sup>-</sup> )	Planar	High-k, Thickness1	No
2	2	p-type (h <sup>+</sup> )	Photogate	ONO Thickness3 ONO Thickness4 ONO Thickness5	No
3	2.16	n-type (e <sup>-</sup> )	Planar	High-k, Thickness2	Yes
4	2.61	n-type (e <sup>-</sup> )	Planar	High-k, Thickness2	No

The photoelement is either a planar photodiode or a vertical photodiode (the photogate pixel), as depicted in “Figure 2.”

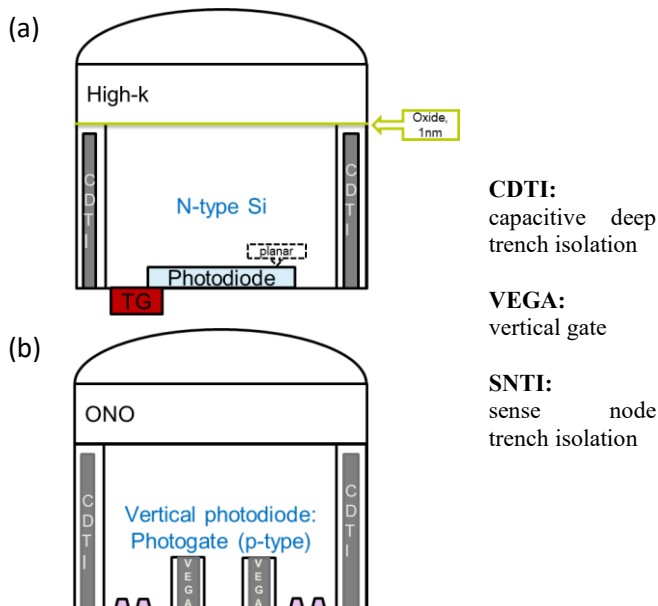


Figure 2 Simplified cross-section of (a) a high-k ARC stack on n-type planar photodiode and (b) an ONO stack on a p-type vertical photodiode (photogate).

### QE measurements bench

Quantum efficiency (QE) is defined as the ratio of the number of collected charges to the number of incident photons. The QE measurements were done thanks to an optical characterization bench that included a monochromator associated to a xenon lamp, emitting light between 200 and 750 nm, Fig.3. QE has been measured down to 200 nm with a sampling step of 10 nm.

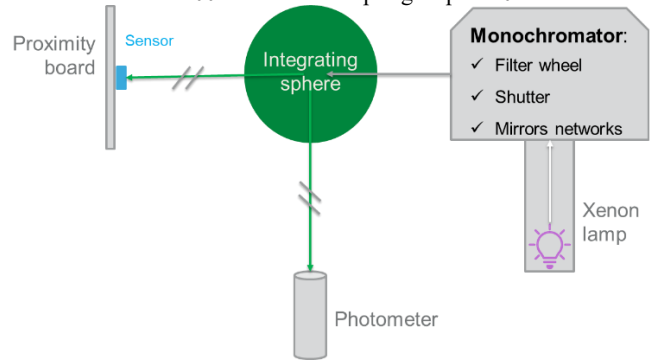


Figure 3 QE bench scheme

### QE experimental results

QE values are normalized to the maximum measured value at a wavelength of 400 nm, corresponding to the “Sample1, High-k Thickness1” records. Fig. 4. depicts the sample’s QE measurements in relative values, in both UV and Vis spectrum. It shows that the sample 1 pixel, has a correct QE response under UV, but the optical response has a significant decrease of about 50% between 400 nm and 200 nm.

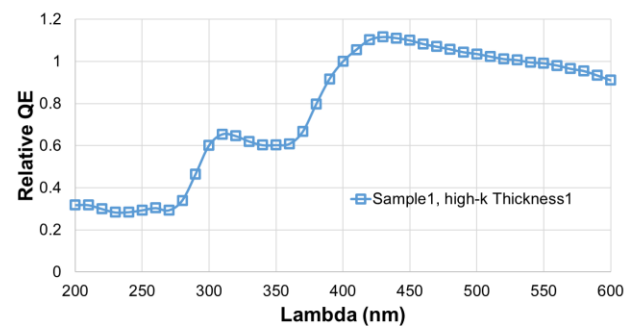


Figure 4 N-type planar photodiode pixel's QE in UV and Vis spectrum

Next Fig. 5a illustrates the impact of the presence of an organic microlens on the QE of sample 3 compared to sample 4: it causes a clear QE loss around 300nm. The thickness of the ARC dielectrics seems to modulate the QE oscillations on wavelengths greater than 300 nm, but does not significantly modulate the QE loss slope under 400nm, as shown in Fig5 b. The type of ARC dielectric (High-k or ONO) has no bearing on the results.

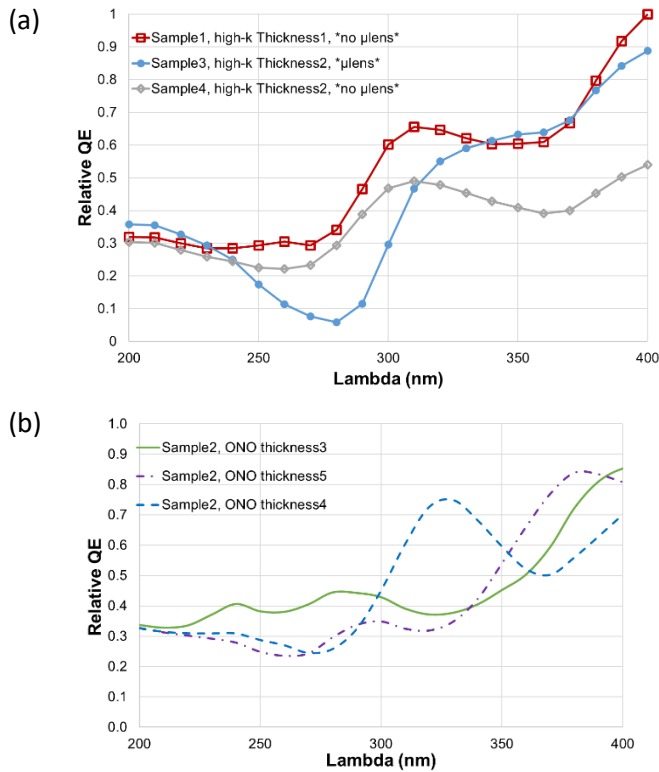


Figure 5 Normalized QE for (a) two N-type planar photodiode pixels for comparison, normalized at 400 nm (b) Sample2 (photogate), with the 3 declinations of ONO

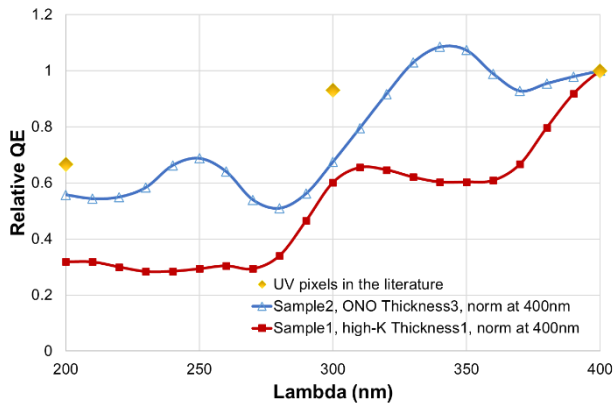


Figure 6 QE of P-type photogate Vs N-type planar photodiode pixel, compared to relative values from the lastly developed UV pixel from the literature [8], normalized at 400 nm

Finally, the relative QE measurements on Fig.6 show that the best performing pixel's technology at  $\lambda=200$  nm -among those in the "Table 1."- is the p-type photogate. The recorded value at 200 nm is equal to the QE value at 400 nm divided by, approximately, 45%. For the best performing measured one at 300 nm, the planar photodiode without microlens, Sample1, Fig.5(a), the QE value has also dropped by more than 30% from 400 nm. This seems quite good, especially if compared to the QE values of one of the latest developed pixels dedicated to UV [8]. The QE value of that last

pixel, at 200 nm, is, roughly, half the QE at 400 nm and is the minimum recorded value of this pixel. As a result, the values of the QE at  $\lambda=200$  nm, particularly for the photogate, are comparable to those reported in the literature.

## ARC optical simulations

### Methodology

Based on the measurement results, it was important to understand the optical behavior of the passivation stack to analyze the measured data. For this, optical simulations were performed to quantify the different stacks' transmittance and reflectance and to see how they impact the QE.

The optical simulations were done using Lumerical, with the "stackrt" function of the software. The input data for these simulations (real & complex values of index) were extracted from ellipsometer data measured in STMicroelectronics facilities on the material of interest (TEOS, SiON, Al<sub>2</sub>O<sub>3</sub>, Ta<sub>2</sub>O<sub>5</sub>, microlenses resist).

### Optical simulations results

All the ARC stacks used in the measured pixels were simulated. Thicknesses get bigger as the thickness number in "Table 1." is incrementing, for the ONO stack, and smaller for the high-K stack.

We observe that the ARC transmission under 300nm seems very good and not depending of the wavelength. It has an impact on the transmission oscillations observed between 300 and 400nm. Next, the nature of ARC dielectric does not seem to play a significant role on the transmission under UV. The modulation of both curves is typical of classical multilayer optical interference peaks, Fig.7.

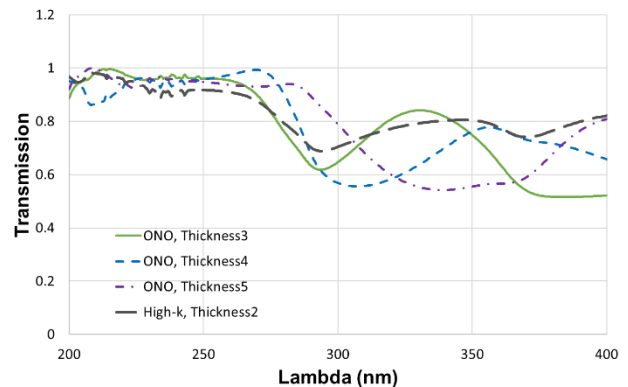


Figure 7 Transmittance simulations of the stack the ONO stacks used on Sample2

Furthermore, the presence of microlenses was simulated to see how much it reduced transmittance, particularly in the UV spectrum. That simulation was done by adding a simple planar stack of the microlens material, to the ARC stack, Fig.8.

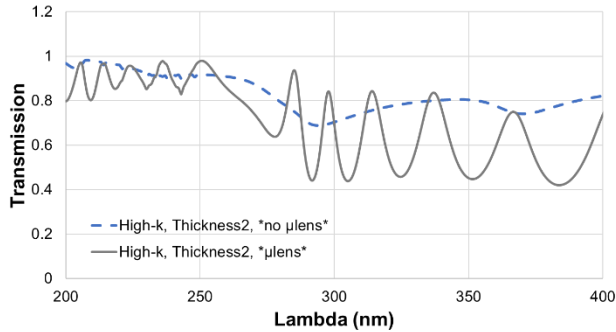


Figure 8 Transmittance simulation of a high-k stack of a measured pixel, without μlens and with the μlens material on

We observe that the presence of the microlens resist induces a strong transmission oscillation, which is a sign of an increased light absorption effect.

## Discussion

First, we can deduce that the QE loss observed for  $\lambda=300$  nm on the sample with microlens resist is the result of the optical transmission loss due to this organic layer, as indicated by the simulation. It should be avoided for UV sensors.

Next, the similar QE behavior between samples with different ARC dielectrics is also consistent with the good transmission under UV of the different stacks.

For the ONO stack and wavelengths under 300 nm, the thickness does not impact the QE performance much, Fig.7: regardless of the stack's thickness, although the transmittance is close to its maximum values, the measured QE is very poor, even though results obtained with the thickness 3 are slightly better. For wavelengths between 300 nm and 400 nm, the measured QE and the simulated transmission look quite similar. Finally, the QE of the measured pixels under UV is significantly lower than in the visible, Fig.4. This is not consistent with the ARC transmission simulation and suggests that the low QE below 300 nm is mainly due to the photocarrier recombination issue close to the Si interface.

To understand the photocarriers recombination issue mentioned above, we can have a brief overview of the defects that can be found at the Si/SiO<sub>2</sub> interface, i.e. between the Si substrate and the first ARC layer.

In fact, the P<sub>b</sub> center defect, the most current electrically active defect in the Si-SiO<sub>2</sub> interface [9] is a Si atom bonded by three other Si atoms and a dangling bond. One of the configurations of this defect is circled with green dashes in the Fig.9. Those defects participate in the trapping and detrapping of carriers and play a role in deteriorating the electrical performance of MOS by increasing the dark current, for example [10]

These interface defects, combined with the low absorption depth in the UV range, are the primary cause of the poor quantum efficiency performance.

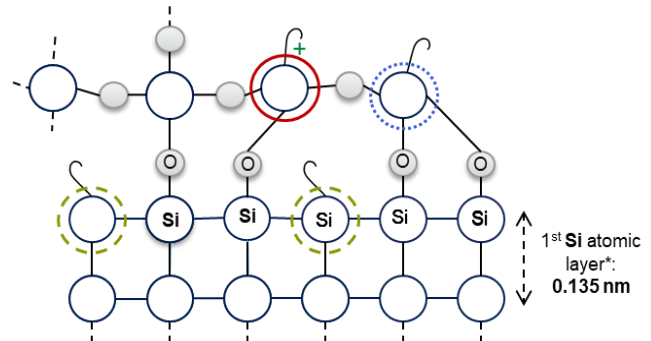


Figure 9 Main defects at the Si-SiO<sub>2</sub> interface, depending on the trivalent Si model, adapted from [9] where the defects in green dashed circle represent interface traps (because of the remaining dangling bond), the blue dotted one is responsible for hole trapping and radiation induced defects and the red solid one represents another hole trap. \*[11]

For a better understanding of the QE, an electrical study should be done to evaluate, for each of the ARC and passivation coatings, how the Si defects prevent the electrons' drift and diffusion.

## Conclusion

All the backside illuminated pixels studied here were developed for Vis and, in some cases, for NIR applications. That's the reason why materials and thicknesses used for passivation and ARC coatings are not tailored for UV. However, these pixels give quite good QE performance under UV, but show a clear signal loss when the wavelength goes down to 200 nm. Thanks to optical simulations performed in the UV range, it seems that the optical stack transmission is quite good, which suggests that the main cause of the low QE is the photocarrier recombination due to the defects at the Si/SiO<sub>2</sub> interface.

Further electrical and optical simulations, planned as the next step of our study, should allow an optimization of the coating to minimize the interface defects and maximize the transmission.

## References

- [1] Okino, T., Yamahira, S., Yamada, S., Hirose, Y., Odagawa, A., Kato, Y., & Tanaka, T. (2018). A real-time ultraviolet radiation imaging system using an organic photoconductive image sensor. *Sensors*, 18(1), 314.
- [2] EHRT, Doris. Deep-UV materials. *Advanced Optical Technologies*, 2018, vol. 7, no 4, p. 225-242.
- [3] WESTHOFF, R. C., BURKE, B. E., CLARK, H. R., et al. Low dark current, back-illuminated charge coupled devices. In : *Sensors, Cameras, and Systems for Industrial/Scientific Applications X*. SPIE, 2009. p. 114-124.
- [4] RYU, K. K., LEITZ, C. W., CLARK, H. R., et al. Oxide-bonded molecular-beam epitaxial backside passivation process for large-format CCDs. In : *Space Telescopes and Instrumentation 2018: Ultraviolet to Gamma Ray*. SPIE, 2018. p. 933-944.
- [5] Hoenk, Michael & Jones, Todd & Dickie, Matthew & Greer, Frank & Cunningham, Thomas & Blazejewski, Edward & Nikzad, Shouleh. (2009). Delta-doped back-illuminated CMOS imaging arrays: Progress and prospects. *Proceedings of SPIE* -

The International Society for Optical Engineering. 7419.  
10.1117/12.832326.

- [6] Peng Sun, Sheng Hu, Wen Zou, Peng-Fei Wang, Lin Chen, Hao Zhu, Qing-Qing Sun, and David Wei Zhang, "Backside passivation for improving the noise performance in CMOS image sensor", *AIP Advances* 10, 045229 (2020) <https://doi.org/10.1063/5.0006700>
- [7] SACCHETTINI, Y., CARRÈRE, J.-P., DOYEN, C., et al. A highly reliable back side illuminated pixel against plasma induced damage. In : 2019 IEEE International Electron Devices Meeting (IEDM). IEEE, 2019. p. 16.5. 1-16.5. 4.
- [8] Sony releases new sensors IMX487, IMX661. (2022, July 5). from [https://image-sensors-world.blogspot.com/2022/07/sony-releases-new-sensors-imx487-imx661.html?lr=1&\\_sm\\_au\\_=iVVVqrQZqJPm53R3cLpsvK618Vf61](https://image-sensors-world.blogspot.com/2022/07/sony-releases-new-sensors-imx487-imx661.html?lr=1&_sm_au_=iVVVqrQZqJPm53R3cLpsvK618Vf61)
- [9] BARBOTTIN, Gérard et VAPAILLE, André. *Instabilities in silicon devices: silicon passivation and related instabilities*. North-Holland, 1986.
- [10] LI, Flora et NATHAN, Arokia. *CCD image sensors in deep-ultraviolet: degradation behavior and damage mechanisms*. Springer Science & Business Media, 2005.
- [11] TSUTSUI, Kazuo, MATSUSHITA, Tomohiro, NATORI, Kotaro, et al. Individual atomic imaging of multiple dopant sites in As-doped Si using spectro-photoelectron holography. *Nano Letters*, 2017, vol. 17, no 12, p. 7533-7538.